Quantitative *In Vivo* Measurement of Gyrification in the Human Brain: Changes Associated with Aging

Vincent A. Magnotta, Nancy C. Andreasen, Susan K. Schultz, Greg Harris, Ted Cizadlo, Dan Heckel, Peg Nopoulos and Michael Flaum

Mental Health Clinical Research Center, The University of Iowa College of Medicine and Hospitals and Clinics, 200 Hawkins Drive, Iowa City, IA 52242, USA

Clinical observation suggests that the aging process affects gyrification, with the brain appearing more 'atrophic' with increasing age. Empirical studies of tissue type indicate that gray matter volume decreases with age while cerebrospinal fluid increases. Quantitative changes in cortical surface characteristics such as sulcal and gyral shape have not been measured, however, due to difficulties in developing a method that separates abutting gyral crowns and opens up the sulci – the 'problem of buried cortex'. We describe a quantitative method for measuring brain surface characteristics that is reliable and valid. This method is used to define the gyral and sulcal characteristics of atrophic and non-atrophic brains and to examine changes that occur with aging in a sample of 148 normal individuals from a broad age range. The shape of gyri and sulci change significantly over time, with the gyri becoming more sharply and steeply curved, while the sulci become more flattened and less curved. Cortical thickness also decreases over time. Cortical thinning progresses more rapidly in males than in females. The progression of these changes appears to be relatively stable during midlife and to begin to progress some time during the fourth decade. Measurements of sulcal and gyral shape may be useful in studying the mechanisms of both neurodevelopmental and neurodegenerative changes that occur during brain maturation and aging.

Introduction

The human cerebral cortex is highly gyrified in comparison with many other species. This high level of gyrification has occurred in concert with an increase in overall cerebral size. The increased degree of folding in the human brain is believed to reflect a need to increase its surface area (and consequently its functional capacity) in response to evolutionary demands, without increasing intracranial size to a degree that would be disproportionate to overall body size (Zilles *et al.*, 1988; Armstrong *et al.*, 1995). Various mechanisms have been proposed to explain the observed patterns of gyrification, ranging from the possibility that they reflect random mechanical buckling to the possibility that they reflect tension-based mechanical processes that reduce axonal length between interactive cortical areas to the shortest possible distance (Caviness, 1975; Van Essen, 1997).

Quantitative measurements of gyrification can potentially provide important information concerning normal brain development and aging, as well as a variety of disease processes. Sulcal and gyral patterns reflect the effects of both maturational and neurodegenerative processes. They may contain clues concerning the relationship between brain maturation or aging and the development or loss of specific mental abilities in healthy normal individuals, as well as the effects of abnormalities due to either genetic regulation or environmental factors. The formation of sulcal and gyral patterns in the brain appears to be a genetically programmed event, which may be partially modified by environmental influences such as general health, nutrition and injury. The surface of the brain is essentially smooth during the sixth month of gestation, and thereafter the complex enfolding that characterizes the adult human brain begins to occur (Ono *et al.*, 1990). The major sulci (e.g. sylvian fissure, central sulcus) form during the sixth and seventh months of fetal life and continue to develop throughout the gestational period and after birth. The pattern of enfolding is an effect of the massive expansion of cortical gray matter (GM) and the development of interconnecting circuits. During early childhood the degree of gyrification, as determined by the gyrification index (GI), stabilizes (Zilles *et al.*, 1988). Changes in gyrification during the young adult years and latter life have not as yet been examined. The extent to which changes in sulcal and gyral shape occur during adult life and to which they are genetically programmed versus environmentally influenced is at present unknown. Information about individual differences in sulcal/gyral shape or patterns may ultimately be informative about brain plasticity and the effects of environmental stimuli or injuries on both brain maturation and degenerative changes associated with aging.

The advent of magnetic resonance imaging (MRI) offers neuroscientists an opportunity to complement labor-intensive post-mortem studies of gyrification with efficient computerized *in vivo* methods in order to study patterns of both brain development and the changes associated with aging. However, characterizing the complex structure of the cortical surface, as visualized by MRI, also presents several challenges. Conventional volume rendering programs provide visually accurate images of the surface of the brain that look very similar to post-mortem tissue. However, they are inadequate for accurately depicting the depths of sulcal invaginations, since the edges of gyral crowns frequently abut one another – the 'problem of buried cortex'. This problem, illustrated in Figure 1, must be solved before accurate measurements can be applied to questions concerning normal development and aging or disease processes. Surface rendering programs that generate a surface mask based solely on the cortical surface can readily distinguish normal brain from grossly atrophic brain (Fig. 1*A* versus *B*), since very atrophic brains have grossly widened sulci, and sulcal GM is therefore exposed. However, they cannot detect sulcal invaginations filled with cerebrospinal fluid (CSF) due to mild atrophy (Fig. 1*C*), since the gyral crowns touch one another and the surface mask appears identical to Figure 1*A*. Nor can they identify deep enfolding occurring as a consequence of an advanced level of gyrification (Fig. 1*D*). Investigations of gyrification require a method to separate abutting gyral crowns and to produce a mask that follows the cortical ribbon into sulci; otherwise Figure 1*B–D* will be indistinguishable. Without a solution of the problem of buried cortex, measurements of gyrification to study normal brain development or aging or specific disease processes may be misleading and potentially meaningless.

This problem with *in vivo* MR-based measurements has been explored both by us and by others (Andreasen *et al.*, 1994;

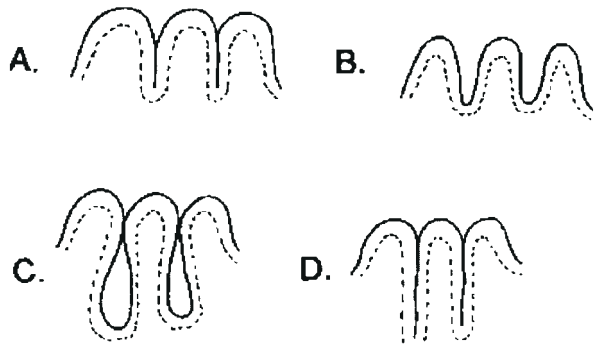

Figure 1. An illustration of the problem of 'buried cortex'. The problem of 'buried cortex' arises when the surface as defined by the mask does not adequately depict the presence of sulci. That is, surface-rendering algorithms will be robust to detecting gross atrophy (*A* versus *B*), but may not detect instances of atrophy where the GM pixels touch one another near the surface but contain CSF in an invagination (*C*, which would appear similar to *A* on the mask). They will also fail to detect instances of deep infolding (*D*), due to a high level of gyrification.

Sisodiya *et al.*, 1996; Cizadlo *et al.*, 1997; Sisodiya and Free, 1997). The solution of Sisidoya *et al.* is to completely remove all cortical GM and to define brain surface based on axonal projections to GM [i.e. white matter (WM) only]. While having the advantage of opening up sulci, this approach has the disadvantage of losing information that is particularly informative about brain development and aging: cortical thickness, potential contributions of neuropil to gyrification, and other aspects of GM. Therefore, we have developed a new method for identifying brain surface (BRAINSURF), which provides an interrelated set of measures that can be used as an index of cortical surface characteristics (Cizadlo *et al.*, 1997). This method opens up sulci to reveal buried cortex through a consistent erosion of cortical GM throughout the entire brain surface. It therefore retains regional information about cortical thickness that can be used to indirectly examine relationships between neuronal density, neuropil and axonal projections. This computationally efficient and fully automated method provides quantitative measurements of surface area, GM depth, and indices of curvature and surface complexity.

We have applied this method to the study of normal aging in a large cohort of healthy volunteers. While there has been relatively extensive study of the relationship between gyrification and normal brain development and evolutionary biology, the changes in gyrification associated with normal aging have not been quantitatively defined. Methods using *in vivo* imaging for the study of aging have emphasized measurement of changes in the relative volume of overall brain tissue or GM, WM and CSF, documenting that brain tissue and GM decrease as a consequence of normal aging while CSF increases (Andreasen *et al.*, 1990; Jernigan *et al.*, 1990; Pfefferbaum *et al.*, 1994; Matsumae *et al.*, 1996). Investigators have also examined whether the changes in brain tissue that occur as a consequence of aging are regionally specific (Raz *et al.*, 1997). While there is little debate as to whether tissue changes occur with aging, very little is known about how these changes affect sulcal and gyral patterns or about the mechanisms that produce such changes. We do not know whether the mechanisms are similar to, or different from, those that affect fetal and childhood neurodevelopment at either the gross or the molecular level. Nor do we know how to define the point at which the ongoing developmental modeling that shapes the brain into the teens and early twenties, such as pruning or 'activity-dependent changes', transform from a 'developmental' to a 'degenerative' process involving neuronal loss, regression of dendritic arborization or decrease in synapses. An easily applied, automated, quantitative measurement of brain surface characteristics is a useful tool for such studies. Consequently, herein we report on both the development of a method and its application to a large cohort of normal volunteers from a broad age range in order to examine the changes in sulcal and gyral anatomy associated with brain aging during the period beginning in the late teens and extending into the early 80s.

Materials and Methods

Initial Study of Atrophic Changes

The initial test of the method is its ability to produce an objective quantitative measurement of the way that gyrification characteristics differ in brains that are considered atrophic versus those that are considered to be normal. Therefore, as a first step, we compared the quantitative measurements generated by BRAINSURF, using brains with normal surface anatomy and brains with a surface that experienced clinicians have rated visually and characterized as moderately to severely atrophic. A total of 18 subjects, nine with notable atrophy and nine normal, were compared for gyral and sulcal curvature, cortical depth and cerebral surface area. The scans were visually rated by two experienced clinicians (N.C.A. and M.F.), who made a consensus rating of atrophy using a 0–5 scale, analogous to the CERAD scale (Davis *et al.*, 1989). The atrophy scale applied was based on anchor points defined by a locally developed photographic atlas. Extreme groups were selected for this substudy, and so the normal subjects all had ratings of 0 or 1, while the atrophic brains had ratings of 4 or 5. (See Fig. 2 for an illustration of a normal versus an atrophic brain.) Atrophy of the cerebral cortex typically results in a widening of the sulcal regions and a decrease in the width of sulci. A distinction between atrophic and non-atrophic brains, as visually identified, was predicted to be described by the automated algorithm as an alteration in radii of curvature, where the gyri increase in curvature (i.e. have a larger positive curvature index) and the sulci decrease in curvature (i.e. have a larger negative curvature index). In addition, the atrophic brains were predicted to have a thinner cortex than the non-atrophic brains.

Changes in Gyrification Associated with Aging

Having used the study of visually rated atrophy as a means of defining the quantitative gyrification characteristics associated with extreme atrophic changes, we then examined changes in gyrification associated with normal aging by measuring cortical surface characteristics in a large sample of healthy normal volunteers spanning a broad age range. We hypothesized that the changes in gyrification associated with increasing age would be similar to those seen in the brains visually rated as atrophic by human observers.

Subjects

We studied the relationship between brain surface features and normal aging in 148 healthy normal individuals recruited from the community by newspaper advertising. They were screened using a structured interview to rule out psychiatric, neurological or general medical disorders, including substance abuse. Eighty-one were male and 67 female. Their mean age was 28.0 (SD 9.8), with a range from 18 to 82. Their mean educational achievement was 14.6 (SD 1.7). In order to examine whether aging changes occur at a steady rate or begin to accelerate at a particular age, we divided our sample by decade into four age groups. We examined the gyral and sulcal curvature and cortical thickness within each group and also compared these values among the groups. In this portion of the analysis the subjects were categorized by age as follows: (i) age <20 years (n = 11); (ii) age 20–29 years (n = 91); (iii) age 30–39 years (n = 35); and (iv) age >40 years (n = 11).

MR Data Acquisition

Images were obtained on a 1.5 Tesla GE Signa MR scanner. Three different sequences were used for each subject. T_1-weighted images, using a spoiled grass sequence, were acquired with the following parameters:

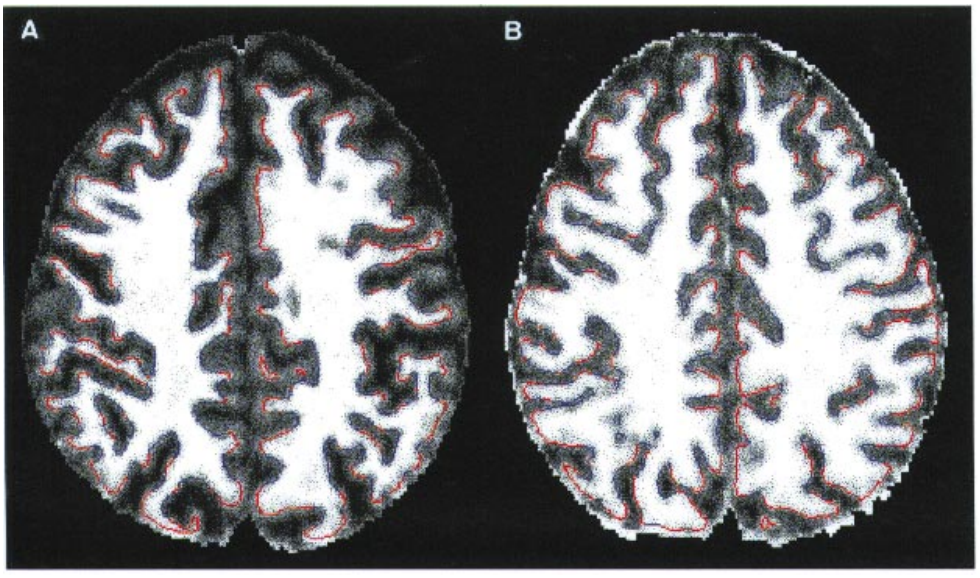

Figure 2. An illustration of a normal brain (*A*) and an atrophic brain (*B*), with the sulci and gyri outlined using BRAINSURF. Note that in the atrophic brain the gyri, shown in red, are more steeply curved and the sulci, shown in blue, are more flattened.

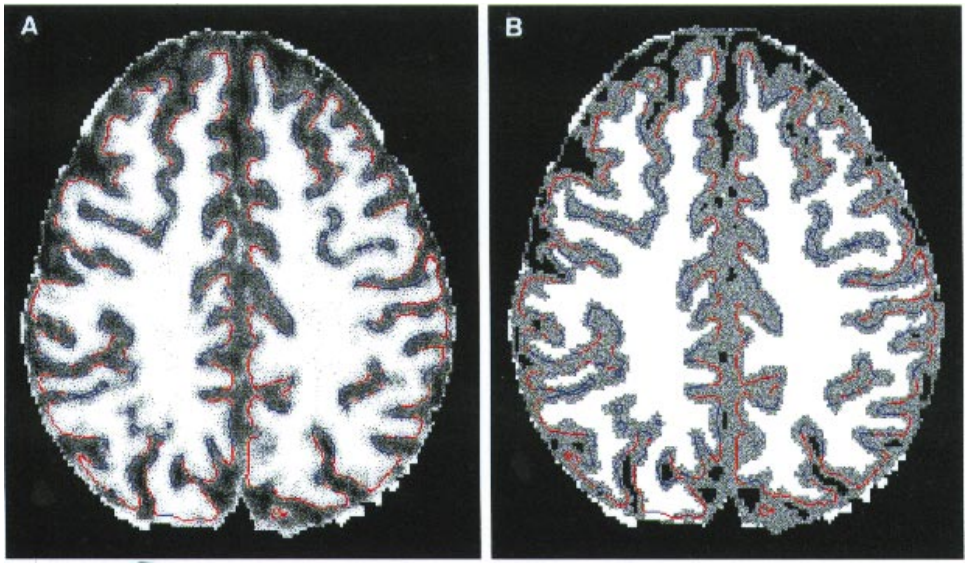

Figure 3. An illustration of the segmented MR images as visualized using the fuzzy (*A*) and sharp (*B*) classifiers. The contours demonstrate the location of the 'pure' GM iso-surface. Visual inspection of (*A*) indicates that the isosurface opens up the sulci with good fidelity but remains within cortical GM. (*B*) has the contours drawn on the corresponding sharply classified image, illustrating that the contours approximate the center of the cortical GM.

1.5 mm coronal slices, 40° flip angle, T_R 24 ms, T_E 5 ms, N_{EX} 2, FOV 26 cm and a 256 × 192 matrix. The PD- and T_2-weighted images were acquired with the following parameters: 3.0 or 4.0 mm coronal slices, T_E 36 ms (for P_D) or 96 ms (for T_2), TR 3000 ms, N_{EX} 1, FOV 26 cm, 256 × 192 matrix and an echo train length = 8**.** After acquisition, all scans were rated for overall quality and for movement artifacts using a 0–4 scale (4 = excellent, 0 = very poor).

Definition of the Cortical Surface

Defining the cortical surface requires two steps in processing the MR data. First, a method for identifying cortical GM must be applied, and a portion of the GM must be removed so that the gyral crowns no longer touch one another and the sulci are opened; this step requires segmenting brain tissue into GM and WM. Our methods for classifying GM and WM have been described previously; these methods have been extensively evaluated for reliability and validity using multiple raters, repeated scans and phantoms (Harris *et al.*, 1999). These methods provide the basis for identifying the cortical surface. In the present report we describe our highly efficient and automated image analysis techniques to define the quantitative characteristics of the cortical surface, such as the degree of curvature of gyri and sulci, as well as methods to visualize the cortical surface.

Segmentation of GM and WM with Correction for Partial Voluming

The first step in the image processing involves segmenting the images. We have developed two methods for segmentation, which differ in their relevant applications. Both use a multispectral discriminant analysis-based segmentation algorithm applied to the three image sequences described above (T_1, T_2 and P_D) (Harris *et al.*, 1997, 1999). One method

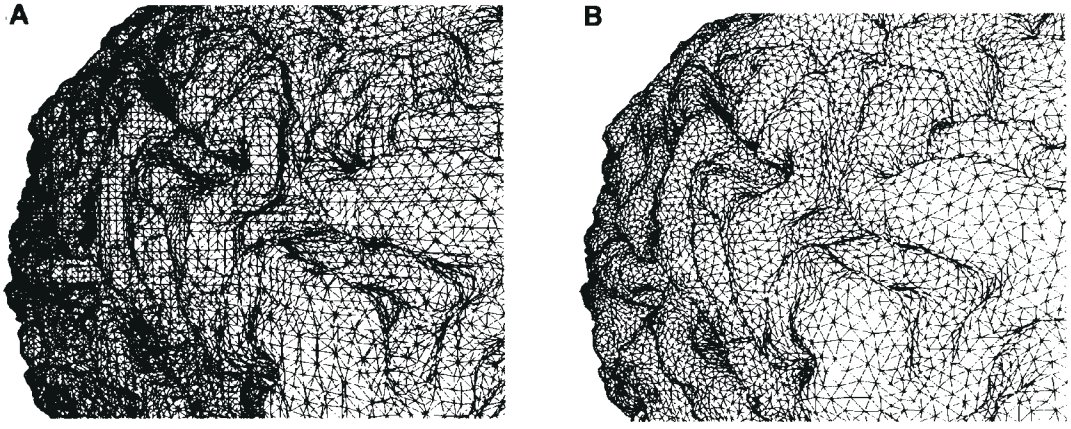

Figure 4. The effects of retiling the cortical iso-surface. (*A*) Original polygonolization consisting of 300 000–500 000 triangles per hemisphere. (*B*) The same surface retiled to ~100 000 triangles per hemisphere.

produces a sharp (discrete) classification of tissue into GM, WM and CSF, while the other uses a fuzzy (continuous) classifier, which corrects for partial voluming. In MRI partial voluming causes the inclusion of both GM and WM (or GM and CSF) in a single voxel, making it difficult to separate them with perfect precision and complicating the identification of GM:CSF boundaries on the brain surface or the GM:WM interface. Our discriminant analysis method permits us to identify the range of voxel intensity values that characterize GM, WM and CSF in our multispectral data. We assign an 8 bit number to each voxel indicating its partial volume tissue content (10–70 for CSF, 70–190 for GM and 190–250 for WM). The sharp classification divides and displays tissue into only three classes, based on the three ranges of voxel intensity, while the fuzzy classification employs and displays the full continuous range of values. Using the fuzzy classifier, however, we can identify the voxel intensity values that will define voxels that contain 'pure' CSF, GM and WM (10, 130 and 250 respectively). In order to define the cortical isosurface to be used in our analyses, we use the value of pure GM, or 130, as a cut-off; this value represents the parametric center of the GM within the cortex and serves as a useful estimate of its physical center. This method for producing the isosurface is illustrated in Figure 3*A*,*B*.

Image Analysis Procedures for Defining the Isosurface

Three steps are applied to create a triangle-based isosurface, using the parametric center of the cortex as the outer boundary of the brain.

1. Polygonalization of Cortical Surface. This technique was initially used to describe geometric modeling techniques for soft objects (Wyvill *et al.*, 1986). The fuzzy image is sampled using points of intersection between small cubes and the chosen surface threshold (i.e. voxel intensity of 130). These intersecting cubes are then used to generate a polygonal patch that reflects the isosurface as it intersects with that small cube. Each patch will then mesh with those generated from neighboring cubes. This method guarantees the creation of an unbroken surface, in which all patches will mesh together.

2. Identification of Cortex. Many small 'noise' surfaces are found in the initial polygonalization. The purpose of this step is to eliminate the surfaces created by image noise and unwanted interior structure caused by blood vessels. A flood fill is used to identify contiguous polygonal surfaces where only the largest of these surfaces are retained. This discrimination is guided by the assumption that the cortex is the largest contiguous surface found.

3. Retiling the Polygonal Surface. To this point, an isosurface is generated with ~300 000–500 000 triangles per hemisphere (see Fig. 4*A*). A retiling algorithm (Turk, 1992) is implemented to reduce the image down to a more manageable size of ~100 000 triangles per hemisphere. This algorithm is initiated by defining a new set of vertices. Random points are then chosen on original surface and their positions are relaxed through point repulsion. Curves can be better preserved by lessening repulsion in highly curved areas. The new surface is created and the topology of the surface preserved by using local retriangulations to add new vertices to existing surface, then old vertices are removed in the same manner. Decimation yields a very similar surface with many fewer and better shaped triangles (see Fig. 4*B*).

Measurement of Parameters

The resulting three-dimensional isosurface approximates the spatial center of the cortex and is used to provide estimates of parameters that are direct or indirect quantitative measurements of gyrification. These measurements are obtained separately for the right and left hemispheres, although we sum them into whole brain measurements in this report for the sake of simplicity. Results of the reliability and validation studies are essentially identical when the data are subdivided into hemispheres.

Sulcal and Gyral Curvature Index

This is an index of how concave or convex each triangle is, as compared to its neighbors up to four triangles away. If points **i** and **j** are the centers of triangles and θ is the angle between the normal to triangle **i** and the vector from **i** to **j**, the curvature measure is the average over all **j** of

$$|\mathbf{ji}|\cos\theta \cdot e^{-|\mathbf{ji}|^2}$$

which is a Gaussian-weighted average emphasizing the nearer neighbors. Convex (i.e. positive) values represent gyri, and concave (i.e. negative) values represent sulci. These are used to provide a curvature index for sulci and gyri for whole brain, for hemispheres and for subregions. The key measures that we report in this study include the whole brain average curvature index for sulci (sulcal curvature index) and for gyri (gyral curvature index).

Surface Area (SA)

This is the straightforward sum of the areas of the triangles making up the surface of the brain. Based on the curvature index, which produces binary positive and negative values for gyri and sulci, the surface area of sulci and gyri can also be calculated.

Cortical Depth

This is an index of the cortical thickness at each triangle. The triangle mesh is located at the position in the cortex which represents pure GM. The distance between each triangle and the GM/WM interface is an index of cortical thickness. Each triangle in the surface is assigned four surface normals, one in the center and one at each corner. The distance to the 50% GM/50% WM location is determined, and the shortest normal is defined as the depth at that triangle. The area of the triangle is used to weight the average calculation. Since cortical depth is based on finding the parametric center of GM, it is approximately half the actual cortical

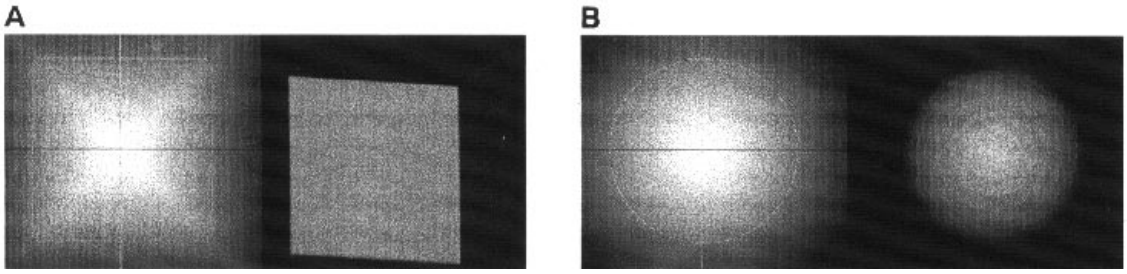

Figure 5. Digital phantoms which were used for validation measurements of thickness and surface area. The images on the left in (*A*) and (*B*) are intensity plots of the three-dimensional simple geometric phantoms. Also shown are the isosurfaces which were defined as part of the analysis.

Table 1
Scan–rescan reproducibilityof measurements

Subject	VOL (cm^3)	% Difference	SA (cm^2)	% Difference	Surface complexity	% Difference	Ave. depth (mm)	% Difference ($T_1 - T_2$)
1A	1428	–0.8	1900	0.3	1498	0.7	1.61	3.1
1B	1439		1895		1487		1.56	
2A	1394	–2.0	1893	–0.6	1516	0.6	2.19	7.3
2B	1422		1905		1507		2.03	
3A	1104	0.24	1522	0.4	1425	0.2	1.91	3.7
3B	1101		1516		1422		1.84	
4A	1171	0.3	1621	–0.7	1459	–0.8	2.05	1.5
4B	1170		1633		1471		2.02	
5A	1251	0.5	1694	1.2	1459	0.9	1.74	0.60
5B	1245		1673		1446		1.73	
6A	1272	–0.2	1579	–5.9	1346	–5.6	1.88	6.4
6B	1275		1672		1422		1.76	
7A	1268	–0.4	1662	2.6	1419	3.0	1.83	–4.9
7B	1273		1618		1377		1.92	
Scan–rescan reliability								
	$R^2 = 0.995$		$R^2 = 0.970$		$R^2 = 0.815$		$R^2 = 0.881$	

depth. In order to obtain a measure of actual cortical depth, the values can be multiplied by two. The data reported in this paper are the values for the parametric center (i.e. half the actual cortical thickness).

Surface Complexity (SC)

An index of surface complexity can be calculated by creating a ratio: cortical surface area divided by the tissue volume to the 2/3 power.

While we report whole brain values in this paper, regional measurements of individual lobes can also be obtained, using an atlas-based automated method (Talairach and Tournoux, 1988; Andreasen *et al.*, 1996).

Reliability and Validity of Measured Parameters

In order to assess the reliability (i.e reproducibility) of the method, we obtained repeated scans for seven individuals. The scans were repeated within a 2 week period after the initial scan. Image acquisition, tissue segmentation, identification of the cortical surface and measurements of the cortical surface (i.e. cortical thickness, surface area and curvature) were identical for the two scans, as described above. Reproducibility (i.e. scan–rescan reliability) was determined by calculating an intraclass correlation coefficient (R^2) for the two sets of measurements. In addition, we also calculated the percentage difference between the two occasions. The results of the reproducibility comparison are given in Table 1, which summarizes brain volume (VOL), surface area (SA), surface complexity, average cortical depth and average curvature indices on each of the two occasions for the seven subjects on whom repeated scans were obtained. In general, the reproducibility is excellent. The intraclass R (R^2) for the various measures is excellent, consistently reaching 0.99. The percentage differences between the two occasions of measurement are also very small, indicating that the method is very stable and reproducible.

In order to test the validity of the method, two simple geometrical digital phantom images were created for the testing of the surface area and depth calculations. Images of these phantoms are shown in Figure 5. The intensity at each voxel was calculated using a function that decreased linearly with distance from the center of the image. The surface generated on one of these images (at a given voxel intensity threshold) was cubical and the other spherical. Two different gradients were used for defining the spheres, effectively yielding different radii. The known surface areas were compared to the measured values using the surface methods described above. The measurements obtained from the spherical and cubical digital phantoms are summarized in Table 2. The surface area calculations are all within close agreement, ≤1%, with the actual values for both the spherical and cubical phantoms. More variation is seen in the depth values. This variation is attributed to the digitization (0–255) of the pixel intensities and to the sharp corners of the cubical phantom. Because the thickness is calculated by using the shortest of the normal vectors, a systematic underestimation will occur in a regularly shaped object such as a sphere.

Table 2
Measurements made from digital phantoms

Phantom	SA ($pixels^2$)	Measured SA ($pixels^2$)	% Difference	Depth (mm)	Measured ave. depth (mm)	% Difference
Cube, 124 × 124	92 256	91 338	–1.0	2.0	2.11	5.3
Sphere, $r = 62.5$	49 087	48 727	–0.7	2.0	1.97	–1.6
Sphere, $r = 31.25$	12 272	12 158	–0.9	2.0	1.94	–3.1

Results

Images of the cortical surface, as visualized by the reconstruction techniques created through BRAINSURF, are shown in Figure 6. Both shaded surface images and reconstructed visual images of the brain surface with color-coded sulci and gyri, as identified by the curvature indices, were created. Visualization of a hemispheric isosurface, using both shading and binary color coding, can be seen in Figure 6. The triangular grid has been shaded in the image on the left, which permits a realistic view of an individual brain and allows for a discriminating inspection of the cortical surface and its gyral patterns. Using BRAINSURF, this surface can be viewed from any angle in real time. Binary curvature images, with convex values colored red and concave colored blue, are also shown on the right. These binary images illustrate that the method can readily distinguish the sulcal and gyral regions with good fidelity.

Comparison of Atrophic versus Non-atrophic Brains

The results of the comparison of atrophic with non-atrophic brains are shown in Table 3. These data indicate a significant difference between the two groups for the gyral and sulcal curvature indices and for average cortical depth. The sulcal and gyral curvature indices differ in opposite fashion when normal

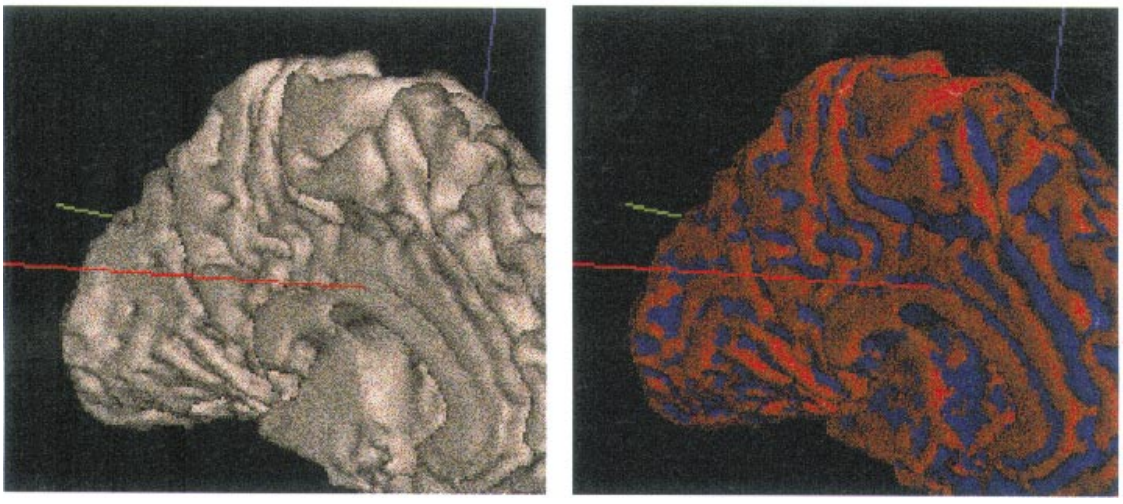

Figure 6. The surface visualization provided by BRAINSURF. The brain surface produced by removing the outer half of the cortex is shown on the left, illustrating how sulci are opened up and 'buried cortex' is eliminated. The colored surface is shown on the right, with sulci shown in blue and gyri in red.

Table 3
Comparison of normal versus atrophic brains

Group	Gyral curvature	Sulcal curvature	Cortical depth (mm)
Normal ($n = 9$)	287.2 ± 5.8	–312.6 ± 6.3	2.07 ± 0.15
Atrophic ($n = 9$)	296.2 ± 3.9	–300.7 ± 4.9	1.89 ± 0.24
Probability > |T|	0.0018*	0.0005*	0.076**

Statistically significant: *two tailed; **one tailed.

Table 4
Relationship between age and sulcal and gyral curvature and cortical thickness

	Mean	SD	Min	Max	R^2	F	P	Spearman r	P
Gyral curvature	289.16	4.38	277.6	300.62	0.233	44.42	0.0001	0.46	0.0001
Sulcal curvature	–309.37	–4.80	–321.81	–294.14	0.250	48.72	0.0001	0.47	0.0001
Cortical depth (mm)	1.97	0.19	1.57	2.48	0.150	25.84	0.0001	–0.50	0.0001

and atrophic brains are compared with one another. The atrophic process causes the gyri to become narrower and more steeply curved, producing an increase in the gyral curvature (i.e. a larger positive curvature index). The atrophic process also leads to a broadening and flattening of the sulci, resulting in a decrease in sulcal curvature (i.e. a larger negative curvature index). Both these differences are highly significant ($P < 0.0018$ and 0.0005 respectively, two tailed). The difference in total cortical depth between the two groups is statistically significant as a one-tailed test (0.035). The groups do not differ in measures of surface complexity or surface area.

Relationship Between Age and Sulcal and Gyral Curvature and Cortical Depth

Using our large sample of MRI scans from 148 normal individuals who represent a broad age range, we plotted the relationship between age and the sulcal and gyral curvature indices, as well as cortical depth, as shown in Table 4 and Figure 7. This analysis permits identification of the changes that occur in the shape of sulci and gyri and in cortical thickness as a consequence of the process of normal aging. Not surprisingly, these changes are similar to those seen when the atrophic and normal brains were compared. That is, during the process of normal aging the sulci and gyri change shape and the cortical mantle diminishes in thickness, in a pattern identical to that seen in atrophic brains. As with the atrophic brains, there were no significant relationships with surface complexity or surface area.

Table 4 shows the mean, standard deviation, minimum and maximum values for sulcal and gyral average curvature and for cortical depth for the 148 individuals whom we have studied. As indicated in that table, the relationship between these variables is highly significant when viewed either from the perspective of an analysis of variance/regression model or when correlation coefficients are examined. The F for all three variables is highly significant ($P < .0001$), and the r^2 ranges from 0.250 to 0.150. Because the data were not normally distributed, the nonparametric Spearman was used to determine correlations. Increasing age has high (and highly significant) positive correlations with age, while cortical depth has a high negative correlation. The slope of these relationships is portrayed graphically in Figure 7.

As these data indicate, the human brain undergoes changes in gyral and sulcal shape and in cortical thickness as a consequence of the aging process. As seen via the measure of cortical depth, the cortical mantle becomes thinner with increasing age, declining from a mean value of ~2 in the 18 year olds to a value of 1.56 in the oldest individual in the sample (an 82 year old). As was seen in the atrophic brains, the sulcal curvature index becomes increasingly larger (i.e. less negative) with increasing age, reflecting the widening of sulci that occurs as a consequence of the GM loss. In corresponding fashion, the gyral curvature index becomes increasingly more positive, reflecting a narrowing of the gyral crowns and a sharpening of the steepness of their curvature.

We also sought to determine whether these changes that occur with aging begin to accelerate at a particular point in time, as a way of addressing the question of when normal maturational processes begin to slow down or stop and when degenerative changes begin. As described above, we subdivided the sample into four age cohorts for these analyses. The values for sulcal, gyral and cortical measures within these categories are summarized in Table 5.

Analysis of the difference between the groups involved a

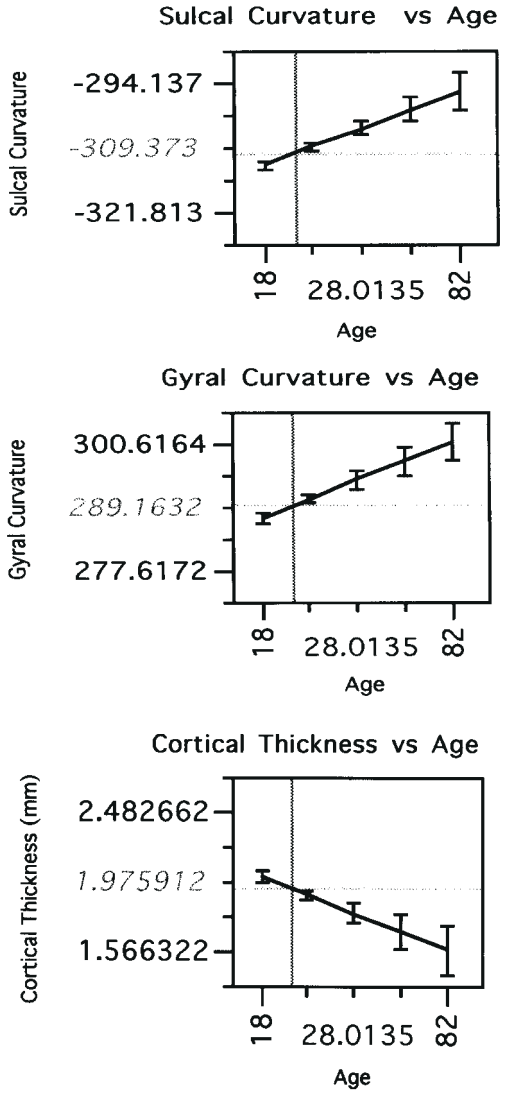

Figure 7. The three key measures of gyrification are plotted against age in a sample of 148 healthy normal volunteers who range in age from 18 to 82. These measures include average sulcal curvature, average gyral curvature and cortical thickness (average depth of the parametric center of the cortex). As portrayed in these graphs, changes occur in the aging brain that reflect the increasing progression of atrophic processes. That is, the sulcal curvature index becomes increasingly more negative, reflecting a flattening and opening up of the sulci; the gyral curvature index becomes increasingly more positive, reflecting a narrowing of the gyral crowns and a sharpening of their curvature; and the cortex becomes progressively thinner.

one-way ANOVA comparing mean values among the four age groups for each of the surface measures. For the gyral curvature measures, there was a significant difference among the groups [$F(147,3) = 12.3$, $P < 0.0001$]. A follow-up test using Tukey–Kramer HSD was performed to assess differences among the individual age groups. This showed that the <20 age group differed in gyral curvature from all other age groups, having the least magnitude of sharpness. Furthermore, the 20–29 age group showed significantly less gyral sharpness than the oldest (>40 group), but did not differ from the other groups. The 30–39 age group differed only from the <20 age group in this measure. These findings are summarized in Figure 8.

A similar procedure was implemented for the sulcal measures. A significant difference was observed across the age groups in the one-way ANOVA [$F(147,3) = 11.7$, $P < 0.0001$]. In the Tukey–

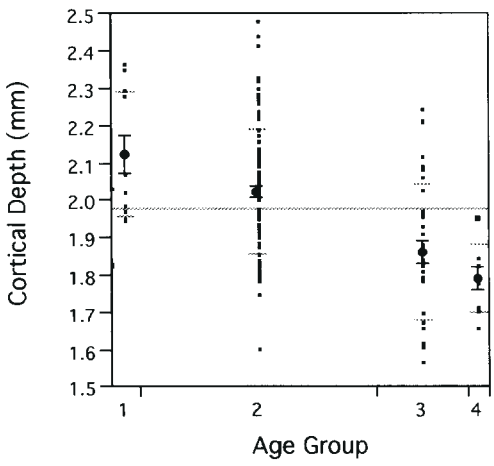

Figure 8. The cortical depth of subjects divided into four age groups: (1) <20; (2) 20–29; (3) 30–39; (4) >40 years old. Cortical depth decreases progressively across the age groups. A between-groups analysis found that the <20 and 20–29 year old groups did not differ in cortical depth, but clearly differed from the 30–39 and >40 age groups. The 30–39 and >40 age groups did not differ from each other.

Kramer HSD between-group analysis, there was a significant difference between the two youngest groups and the two oldest groups (i.e. between those <30 and those >30) but no other group differences. For the cortical depth measures, the ANOVA demonstrated significant differences among the four groups [$F(147,3) = 14.01$, $P < 0.0001$]. Again, there was a significant difference between the two youngest (<30) age groups and the two older (>30) groups. These results are summarized in Figures 9 and 10. More variability is seen in the older age groups than in the younger ones for all three measures (i.e. sulcal and gyral curvature and cortical depth), suggesting that there may be more individual differences associated with the aging process than with earlier developmental processes.

Because there is some indication that men and women differ in progression of changes related to aging (Andreasen *et al.*, 1990; Gur *et al.*, 1991), we also examined age by gender interactions using ANOVA. While (as expected) the ANOVA showed highly significant age effects for sulcal curvature [$F(147,1) = 47.59$, $P < 0.0000$] and gyral curvature [$F(147,1) = 42.49$, $P < 0.0000$], no gender effects or age by gender interactions were significant for these two measures. On the other hand, the ANOVA for cortical depth had a strongly significant age effect [$F(147,1) = 30.88$, $P < 0.0000$], a significant age by gender interaction [$F(147,1) = 5.54$, $P < 0.02$] and a trend level significance for gender effect [$F(147,1) = 3.18$, $P < 0.09$]. Because of this significant interaction, we examined the slope of the regression lines for the two genders, which confirmed that cortical thinning progresses more rapidly in males ($r^2 = 0.26$) than females ($r^2 = 0.08$).

Discussion

The study of gyrification via post-mortem techniques has already taught us a great deal about both the phylogeny and the ontogeny of human brain (Zilles *et al.*, 1988; Armstrong *et al.*, 1995). The challenge that we now confront is to adapt these methods to *in vivo* studies and to explore normal brain development and aging, structure–function relationships and the nature of various disease processes that may have subtle manifestations in gyrification. In this study we have developed a quantitative automated method to achieve *in vivo* measurement of sulcal and gyral characteristics and have applied it to the study of atrophic

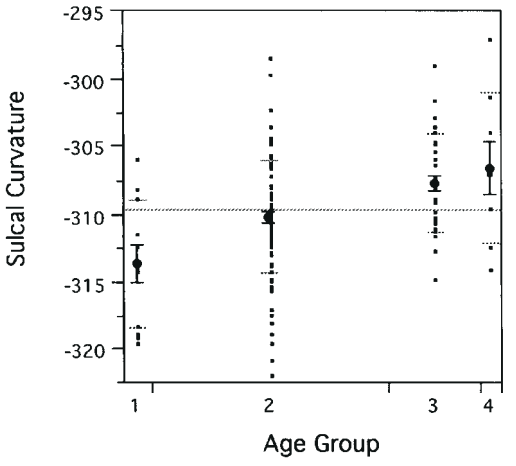

Figure 9. The sulcal curvature measures of subjects divided into four age groups: (1) <20; (2) 20–29; (3) 30–39; (4) >40 years old. Sulcal curvature becomes progressively less negative across the age groups. A between-groups analysis found that the <20 age group differed from the 30–39 and >40 age groups. The 30–39 and >40 age groups did not differ from each other, nor did the <20 and 20–29 year old group.

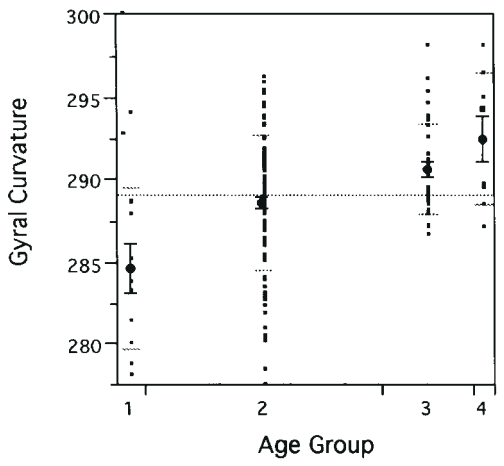

Figure 10. The gyral curvature of subjects divided into four age groups: (1) <20; (2) 20–29; (3) 30–39; (4) >40 years old. Gyral curvature decreases progressively across the age groups. A between-groups analysis found that the <20 year old group differed from all other groups. The 20–29 year old group differed from the <20 and >40 age groups. The 30–39 year old group differed only from the <20 group.

changes and normal aging. To our knowledge, this is the first study to examine the changes in surface characteristics of the cerebral cortex that occur with aging by using quantitative measures of sulcal and gyral shape.

Several needs must be met for successful quantitative *in vivo* studies of brain surface anatomy. First, methods must be developed to identify a brain surface mask that is not confounded by the 'problem of buried cortex' secondary to touching gyral crowns. Second, the methods must be fully automated, because of the large volume of data inherent in MR imaging, making it important to develop computationally efficient approaches that can be quickly executed in large samples. Third, the methods must have demonstrated reliability and validity. Our method meets these three goals and compares favorably with other existing MR-based methods (Jouandet *et al.*, 1989; Sereno *et al.*, 1995; Sisodiya *et al.*, 1996, 1997; Free *et al.*, 1996). The method removes the outer half of the cortex and thereby opens up the sulci, creating a mask of the brain surface that accurately reflects gyral patterns and yet also retains regional information about cortical thickness. It is fully automated and can be used to analyze very large samples rapidly and efficiently, as is demonstrated in the evaluation of gyrification and aging in 148 individuals that we have reported herein. As currently implemented, minimal operator intervention is needed to complete the various steps involved, beginning with brain removal (executed by a neural net), continuing through GM/WM/CSF segmentation, and ending with the measurement of surface characteristics of whole brain, hemispheres or lobes. The absence of operator intervention in the execution of the various measures ensures a high level of reliability. The method has been shown to be reproducible over time, and has been validated by studies with phantoms.

The numerical values produced by this method correspond well with those produced in post-mortem studies or other MR-based methods. For example, the value for surface area reported by Sisodiya *et al.* (1996), ~1627 cm^2, serves as a lower limit for the measurements made here (1516–1905 cm^2). Other estimates taken from post-mortem specimens, 1360–1644 cm^2 (Henerey and Mayhew, 1989), indicate that the values estimated by our *in vivo* method are slightly larger. This difference is probably explained by the combined factors of shrinkage due to fixation and to aging changes in the elderly samples used in post-mortem studies. Further, the cortical depth measurements are largely dependent on where the cortical surface is defined. For this work, the parametric center of the cortex was chosen and a mean GM cortical thickness of 1.87 mm was found, averaged over the six subjects reported in Table 3. Because our measure at the center of the cortex represents the half-width of the cortex, these values should be an estimated 50% of *in vivo* cortical thickness and more than twice the values measured from post-mortem data. Reported cortical thicknesses from post-mortem data are in the range of 1.3–4.5 mm (von Economo, 1929; Rockel *et al.*, 1980; Henery and Mayhew, 1989). *In vivo* MR-based measurements from Sisodiya *et al.* (1996) were reported to have a mean thickness of 3.2 mm.

Applying this method to obtain measurements of atrophic changes in sulcal and gyral curvature, we have found that brains visually classified by clinicians as 'atrophic' have quantifiable characteristic features. Specifically, atrophic gyri have a diminution in their rounded curvature and become more sharply and steeply curved, giving them a larger (more positive) gyral curvature index. Atrophic sulci, on the other hand, become less curved and more flattened, producing a larger (less negative) sulcal curvature index. These two indices can be considered to provide a quantitative index of the degree of atrophy.

When these indices are measured in a large sample of normal individuals ranging in age from 18 to 82, we have found that they show changes that appear to reflect an increase in atrophic processes with increasing age: strong positive correlations between sulcal and gyral curvature and age and a strong negative correlation between cortical thickness and age. These correlations suggest that age accounts for ~25% of the variance in sulcal and gyral surface characteristics and in cortical depth. Although this is the first study to examine sulcal and gyral shape in relation to age, it is consistent with other studies that have used MR to examine changes that occur with age in the volume of GM, WM and CSF. These studies have shown that as age increases, brain tissue decreases and CSF increases (Pfefferbaum *et al.*, 1986;

Andreasen *et al.*, 1990; Jernigan *et al.*, 1990; Gur *et al.*, 1991). GM in particular appears to decline as a consequence of the aging process (Pfefferbaum *et al.*, 1994; Matsumae *et al.*, 1996). Further, some regions appear to be more vulnerable to GM loss, particularly the prefrontal cortex (Raz *et al.*, 1997).

Several key questions arise concerning the mechanisms and meaning of these observations. If aging is associated with GM loss, cortical thinning, and changes in gyral and sulcal shape that appear quantitatively atrophic, when does this process begin? When do normal maturational processes end or stabilize, and when do regressive changes reflecting tissue loss begin? Several previous studies, including our own, have suggested that tissue volume remains relatively stable from the mid-twenties to some time in the forties, that the regressive changes begin during the fifth or sixth decade of life, and that males may begin to show regressive changes earlier than females (Andreasen *et al.*, 1990; Gur *et al.*, 1991; Raz *et al.*, 1993; Cowell *et al.*, 1994; Matsumae *et al.*, 1996). Coffey *et al.* (1992) examined a sample of 76 adults from young adulthood to late life; they reported the odds ratio of ventricular enlargement at age 40 to be 1.0, increasing by 7.7% each year to 2.22 by the ninth decade of life. Similarly, most studies examining CSF measures have largely not identified changes before the age of 40.

These earlier studies have all used volume of CSF, GM or total brain tissue as their primary measures. In this study, using indices of sulcal and gyral shape, we found significant differences associated with aging occur across four age cohorts, which include the late teens, the twenties, the thirties and the over-forties. Our measures of sulcal and gyral curvature and cortical thickness suggest that a break in the pattern of changes seems to occur between the twenties and the thirties. Although a similar pattern of change occurs in all four age cohorts, the process appears to stabilize after the age of 30. The mechanism behind this pattern cannot be determined from MR data of this type, but the occurrence of changes in gyral shape and cortical thickness in the teens and early twenties suggests a neurodevelopmental process such as pruning. The changes in the later two cohorts are more likely to be due to a regressive process. The fact that the cohort in their thirties do not differ significantly from the over-forties cohort suggests that this process may be relatively stable during midlife. This is consistent with primate studies, indicating that synaptogenesis stabilizes during adulthood and remains stable throughout much of adult life (Bourgeois *et al.*, 1994). The sample of individuals >50 is relatively small, however, and so the changes that occur in the 'young elderly' and the 'old elderly' cannot be mapped in detail from these data in order to determine precisely when or if changes begin to accelerate. Our analysis of gender effects using measures of sulcal and gyral curvature did not reveal significant gender by age interactions, although they did indicate a significant age by gender interaction for cortical depth, with males having a more rapid progression of cortical thinning than females, a finding consistent with earlier reports of gender differences in aging. Our sample is at present too small to determine the precise age at which this progression accelerates in males.

The present study has some obvious limitations. First, it is purely descriptive: it tells us *what* happens, but not *why* it happens. The decreasing cortical thickness associated with increasing age, taken in association with the other studies reporting decreased GM volume with increasing age, indicates that the changes primarily affect cortical GM. But we cannot determine whether these changes reflect developmental process such as pruning (in the younger individuals) or degenerative ones such neuronal loss or decrease in neuropil (in the older individuals). The effects on sulcal and gyral shape are presumably secondary to the changes in GM, but we also cannot determine whether these reflect simple mechanical processes (e.g. shrinking and 'caving in') or whether they represent a more active process effected by changes in axonal connectivity between regions. Nor can we determine the cell or molecular biology of these changes. Finally, the purely descriptive results are based on the cross-sectional analysis of a large sample from a relatively broad age range; they are therefore potentially subject to age-cohort effects that might differentially affect the brain in younger versus older individuals, such as nutrition. We also did not have a large enough older sample to examine gender effects or aging changes in the sixties or seventies. Ideally, within-subject longitudinal studies of aging in both men and women are needed, although these are logistically extremely difficult to execute, particularly in a field where technology changes relatively rapidly.

Subsequent studies are needed to address the significance of these findings. This study and the others that have demonstrated aging changes in the cerebral cortex raise many important questions. Are these regressive changes associated with declining mental functions? What are the molecular and cellular mechanisms that produce these changes? Why is there greater variability in these cortical measures in older individuals than in younger ones? Can protective factors be identified that slow the changes, or vulnerability factors that worsen the changes? What patterns are observed in disease processes such as schizophrenia? The ability of measurements of sulcal and gyral shape to separate atrophic from normal brains and to detect subtle changes associated with aging suggests that they will be useful in future studies designed to address these questions.

Notes

This research was supported in part by NIMH grants MH31593, MH40856, and MHCRC43271; a Research Scientist Award, MH00625; and an Established Investigator Award from NARSAD.

Address correspondence to Vincent A. Magnotta, Mental Health Clinical Research Center, The University of Iowa College of Medicine and Hospitals and Clinics, 200 Hawkins Drive, Iowa City, IA 52242, USA. Email: vincent-magnotta@uiowa.edu.

References

Andreasen NC, Swayze VW, Flaum M, Yates WR, Arndt S, McChesney C (1990) Ventricular enlargement in schizophrenia evaluated with computed tomographic scanning: effects of gender, age, and stage of illness. Arch Gen Psychiat 47:1008–1015.

Andreasen NC, Harris G, Cizadlo T, Arndt S, O'Leary D, Swayze V, Flaum M (1994) Techniques for measuring sulcal/gyral patterns in the brain as visualized through magnetic resonance scanning: BRAINPLOT and BRAINMAP. Proc Natl Acad Sci USA 90:93–97.

Andreasen NC, Rajarethinam R, Cizadlo T, Arndt S, Swayze VW II, Flashman LA, O'Leary DS, Ehrhardt JC, Yuh WTC (1996) Automatic atlas-based volume estimation of human brain regions from MR images. J Comput Assist Tomogr 20:98–106.

Armstrong E, Schleicher A, Omran H, Curtis M, Zilles K (1995) The ontogeny of human gyrification. Cereb Cortex 1:56–63.

Bourgeois JP, Goldman-Rakic PS, Rakic P (1994) Synaptogenesis in the prefrontal cortex of rhesus monkeys. Cereb Cortex 4:78–96.

Caviness VS, Jr (1975) Mechanical model of brain convolutional development. Science 189:18–21.

Cizadlo T, Harris G, Heckel D, Flaum M, Christian B, O'Leary DS, Andreasen NC (1997) An automated method to quantify the area, depth, and convolutions of the cerebral cortex from MR data: ('BRAINSURF'). NeuroImage 5:402.

Coffey CE, Wilkinson WE, Parashos IA, Soady SAR, Sullivan RJ, Patterson LJ, Figiel GS, Webb MC, Spritzer CE, Djang WT (1992) Quantitative

cerebral anatomy of the aging human brain: a cross-sectional study using magnetic resonance imaging. Neurology 42:527–536.

Cowell P, Turetsky BI, Gur RC, Grossman RI, Shtasel DL, Gur RE (1994) Sex differences in aging of the human frontal and temporal lobes. J Neurosci 14:4748–4755

Davis P, Gado M, Kuman A, Gray L, Maravilla K, Jolesz F, Albert M, George AE (1989) CERAD neuroimaging protocol for the assessment of Alzheimer's disease. St Louis, Consortium to Establish a Registry for Alzheimer's Disease

Free SL, Sisodiya SM, Cook MJ, Fish DR, Shorvon SD (1996) Three-dimensional fractal analysis of the white matter surface from magnetic resonance images of the human brain. Cereb Cortex 6:830–836; 1047–3211.

Gur RC, Mozley PD, Resnick SM, Gottleib GL, Kohn M, Zimmerman R, Herman G, Atlas S, Grossman R, Beretta D, Erwin R, Gur RE (1991) Gender differences in age effect on brain atrophy measured by magnetic resonance imaging Proc Natl Acad Sci USA 88:2845–2849

Harris G, Andreasen NC, Cizadlo T, Bailey J, Bockholt J, Travis K, Arndt S (1997) Improving tissue segmentation in magnetic resonance imaging: multiple pulse sequences and automated training class selection. NeuroImage 5:402.

Harris G, Andreasen NC, Cizadlo T, Bailey J, Bockholt HJ, Magnotta V, Arndt S (1999) Improving tissue classification in magnetic resonance imaging: a three-dimensional multispectral discriminant analysis method with automated training class selection. J Comput Assist Tomogr (in press).

Henery CC, Mayhew TM (1989) The cerebrum and cerebellum of the fixed human brain: efficient and unbiased estimates of volumes and cortical surfaces areas. J Anat 167:167–180.

Jernigan TL, Press GA, Hesselink JR (1990) Methods for measuring brain morphologic features on magnetic resonance images: validation and normal aging. Arch Neurol 47:27–32.

Jouandet M, Tramo M, Herron D, Hermann A, Loftus W, Bazell J, Gazzaniga M (1989) Brainprints: computer-generated two-dimensional maps of the human cerebral cortex *in vivo*. J Cogn Neurosci 1:88–117.

Matsumae M, Kikinis R, Morocz IA, Lorenzo AV, Sandor T, Albert MS, Black PM, Jolesz FA (1996) Age-related changes in intracranial compartment volumes in normal adults assessed by magnetic resonance imaging J Neurosurg 84:982–991.

Ono M, Kubic S, Abernathy C (1990) Atlas of the cerebral sulci. New York: Thieme.

Pfefferbaum A, Zatz LM, Jernigan TL (1986) Computer-interactive method for quantifying cerebrospinal fluid and tissue in brain/CT scans. J Comput Assist Tomogr 10:571–578.

Pfefferbaum A, Mathalon DH, Sullivan EV, Rawles JM, Zipursky RB, Lim KO (1994) A quantitative magnetic resonance imaging study of changes in brain morphology from infancy to late adulthood. Arch Neurol 51:874–887.

Raz N, Torres IJ, Spencer WD, Baertschie JC, Millman D, Sarpel G (1993) Neuroanatomic correlates of age-sensitive and age-invariant cognitive abilities: an *in vivo* MR investigation. Intelligence 17:407–422.

Raz N, Gunning FM, Head D, Dupuis JH, McQuain J, Briggs SD, Loken WJ, Thornton AE, Acker JD (1997) Selective aging of the human cerebral cortex observed *in vivo*: differential vulnerability of the prefrontal gray matter Cereb Cortex 7: 268–282.

Rockel AJ, Hiorns RW, Powel TP (1980) The basic uniformity in structure of the neocortex. Brain 103:221–224.

Sereno MI, Dale AM, Reppas JB, Kwong KK, Belliveau JW, Brady TJ, Rosen BR, Tootell RB (1995) Borders of multiple visual areas in humans revealed by functional magnetic resonance imaging. Science 268:889–893.

Sisodiya S, Free S (1997) Disproportion of cerebral surface areas and volumes in cerebral dysgenesis: MRI-based evidence for connectional abnormalities. Brain 120:271–281.

Sisodiya S, Free S, Fish D, Shorvon S (1996) MRI-based surface area estimates in the normal adult human brain: evidence for structural organisation. J Anat 188:425–438.

Talairach J, Tournoux P (1988) Co-planar stereotaxic atlas of the human brain. New York: Thieme.

Turk G (1992) Re-tiling polygonal surfaces. Comput Graphics 26:55–64.

Van Essen D (1997) A tension-based theory of morphogensis and compact wiring in the central nervous system. Nature 385:313–318.

von Economo C (1929) The cytoarchitectonics of the human cerebral cortex. London: Oxford University Press.

Wyvill G, McPheeters C, Wyvill B (1986) Data structures for soft objects. Vis Comput 2:227–234.

Zilles K, Armstrong E, Schleicher A, Kretschmann HJ (1988) The human pattern of gyrification in the cerebral cortex. Anat Embryol 179: 173–179.